Electronic Supplementary Material (ESI) for Organic Chemistry Frontiers.


# Support Information

**New multifunctional fluorescent molecule for highly efficient nondoped deep-blue electrofluorescence with high color-purity and efficient phosphorescent OLEDs**

Lei Xu,‡[a] Mizhen Sun,‡[a] Yannan Zhou,[a] Jingli Lou,[a] Mingliang Xie,[a] Zipeng Li,[a] Qikun Sun,[a] Yuyu Pan,[b] Shanfeng Xue[a]* and Wenjun Yang[a]

[a.] Key Laboratory of Rubber-Plastics of the Ministry of Education, School of Polymer Science & Engineering, Qingdao University of Science and Technology, 53-Zhengzhou Road, Qingdao 266042, China.

[b.] School of Petrochemical Engineering, Shenyang University of Technology, 30 Guanghua Street, Liaoyang, 111003, China.

‡ Lei Xu and Mizhen Sun contributed equally to this work.

*Corresponding author E-mail: sfxue@qust.edu.cn

## Contents

# Contents

## SI-1. Measurements

**Photophysical Measurements** UV−vis absorption spectra were recorded on a Hitachi U-4100 spectrophotometer. Fluorescence measurements were recorded on a Hitachi F-4600 spectrophotometer. The photoluminescence (PL) efficiencies in THF, films and solid state，low temperature fluorescence and phosphorescence spectra were measured with a FLS980 spectrometer. The lifetimes of solid state and film state were measured on an Edinburgh FLS-1000 spectrometer with an EPL-375 optical laser.

**Thermal Stability Measurements** Thermal gravimetric analysis was undertaken on a Perkin-Elmer thermal analysis system from 30 to 650 °C at a heating rate of 10 K/ min and a nitrogen flow rate of 80 mL/min. Differential scanning calorimetry (DSC) analysis was carried out using a NETZSCH (DSC-204) instrument from 30 to 450 °C at a heating rate of 10 K/min while flushing with nitrogen.

**Cyclic voltammetry measurements** Cyclic voltammetry (CV) was performed using a BAS 100W (Bioanalytical Systems), using a glass carbon disk (diameter =3 mm) as the working electrode, a platinum wire with a porous ceramic wick as the auxiliary electrode, and $Ag/Ag^+$ as the reference electrode standardized by the redox couple ferrocenium/ferrocene. Anhydrous *N*,*N*-dimethylformamide (DMF) and dichloromethane ($CH_2Cl_2$) containing 0.1 M tetrakis(n-butyl)-ammonium hexafluorophosphate ($NBu_4PF_6$) as the supporting electrolyte were used as solvents under a nitrogen atmosphere. All solutions were purged with a nitrogen stream for 10 min before measurements. The procedure was performed at room temperature, and a nitrogen atmosphere was maintained over the solution during measurements. A scan rate of 50 mV $s^{-1}$ was applied.

**Lippert-Mataga model** The influence of solvent environment on the optical property of our compounds can be understood using the Lippert-Mataga equation, a model that describes the interactions between the solvent and the dipole moment of solute:

$$hc(\upsilon_a - \upsilon_f) = hc(\upsilon_a^0 - \upsilon_f^0) - \frac{2(\mu_e - \mu_g)^2}{a^3} f(\varepsilon, n) \quad (1)$$

where $f$ is the orientational polarizability of solvents, $\mu_e$ is the dipole moment of excited state, $\mu_g$ is the dipole moment of ground state; $a$ is the solvent cavity (Onsager) radius, $\varepsilon$ and $n$ are the solvent dielectric and the solvent refractive index, respectively.

**The EQE measurement method for the non-doped device** The measured parameters included luminance, current and EL spectrum. EQE was calculated according to the formula below:

$$EQE = \frac{\pi \cdot L \cdot e}{683 \cdot I \cdot h \cdot c} \cdot \frac{\int_{380}^{780} I(\lambda) \cdot \lambda d\lambda}{\int_{380}^{780} I(\lambda) \cdot K(\lambda) d\lambda} \quad (2)$$

where $L$ (cd m$^{-2}$) is the total luminance of device, $I$ (A) is the current flowing into the EL device, λ (nm) is EL wavelength, I(λ) is the relative EL intensity at each wavelength and obtained by measuring the EL spectrum, $K$(λ) is the Commision International de L'Eclairage chromaticity (CIE) standard photopic efficiency function, $e$ is the charge of an electron, $h$ is the Planck's constant, c is the velocity of light.

**The radiative exciton ratio of the device** The theoretical value of the radiative exciton ratio was calculated by the following equation:

$$EQE = \gamma \times \phi_{PL} \times \eta_S \times \eta_{out} \quad (3)$$

where EQE is the external quantum efficiency; $\gamma$ is the carrier recombination efficiency, which in the ideal case is supposed to be unity if the injected holes and electrons are fully recombined and degrade to excitons in the emissive layer, $\Phi_{PL}$ is

photoluminescence efficiency of the emission layer (~57% for DTPCZTZ film); $\eta_s$ is the radiative exciton ratio; and $\eta_{out}$ is the light out-coupling efficiency (20%).

## SI-2 Supporting Figures

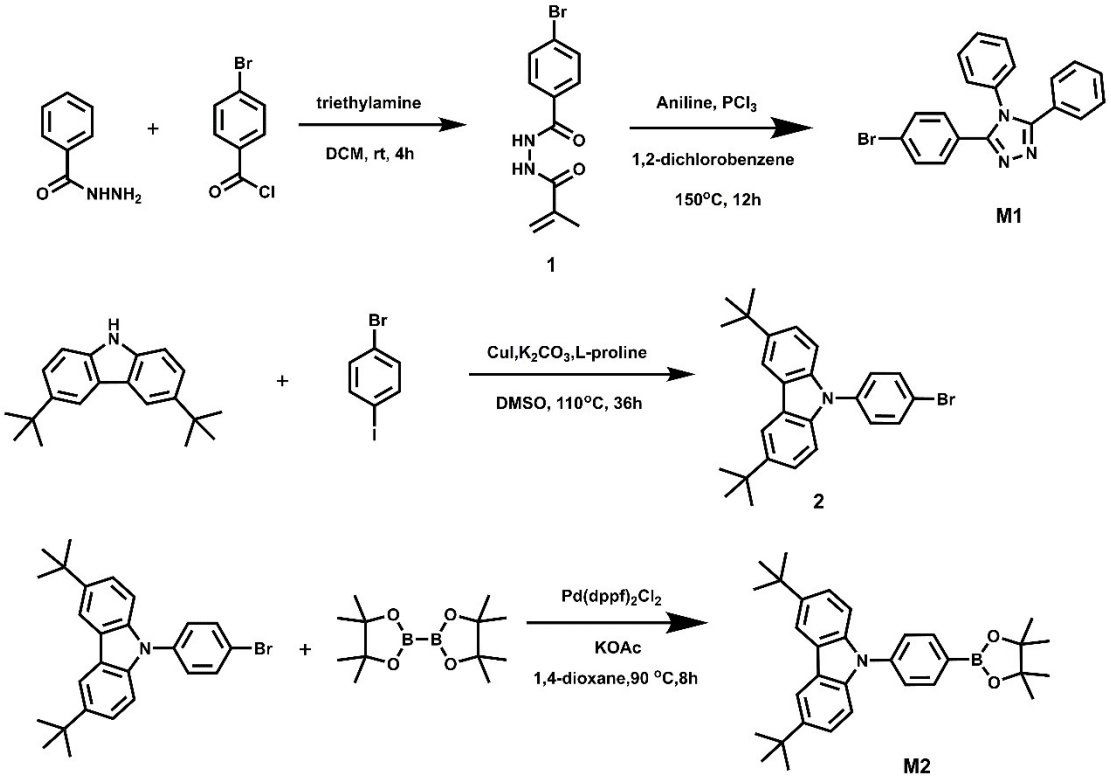


**Scheme S1.** Molecular structure and synthetic route to DTPCZTZ.

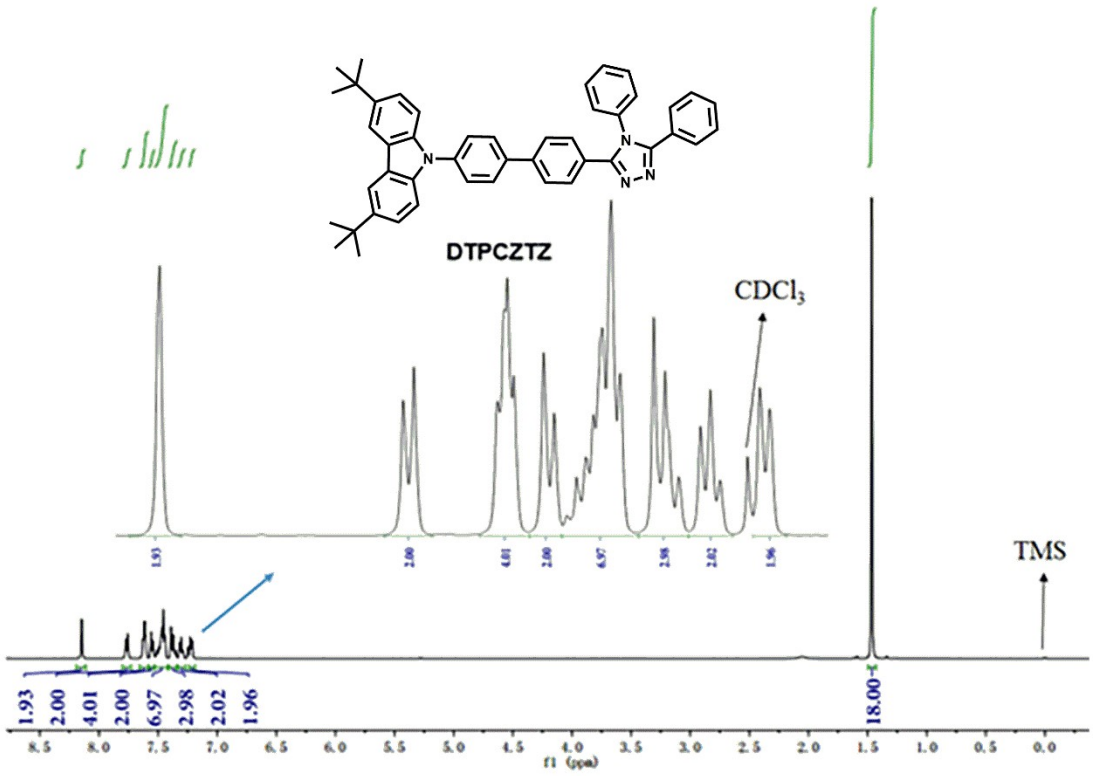


**Figure S1.** $^{1}$H-NMR Spectrum of DTPCZTZ in $CDCl_3$.

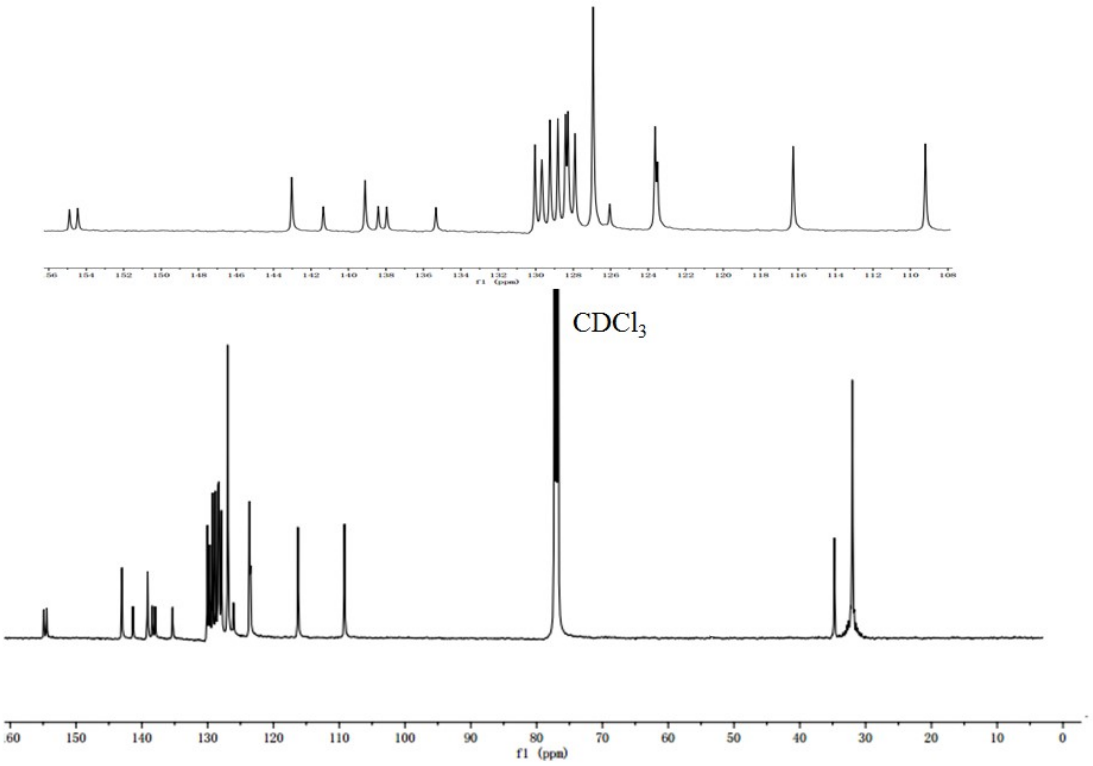


**Figure S2.** $^{13}$C-NMR Spectrum of DTPCZTZ in $CDCl_3$.

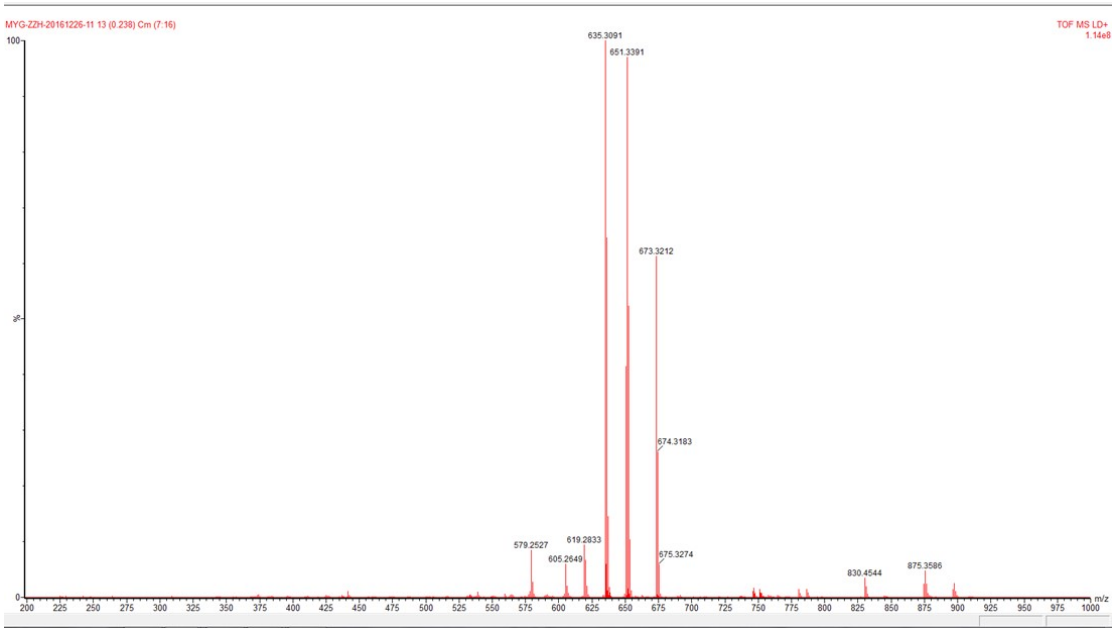


**Figure S3.** The time-of-flight mass spectrum of DTPCZTZ.

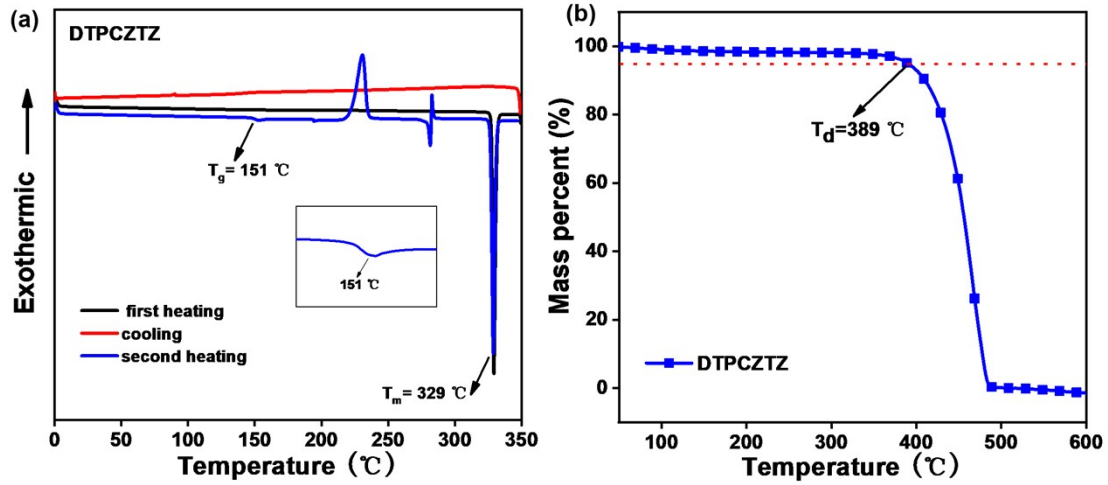


**Figure S4**. a)TGA curve and b)DSC curve of DTPCZTZ.

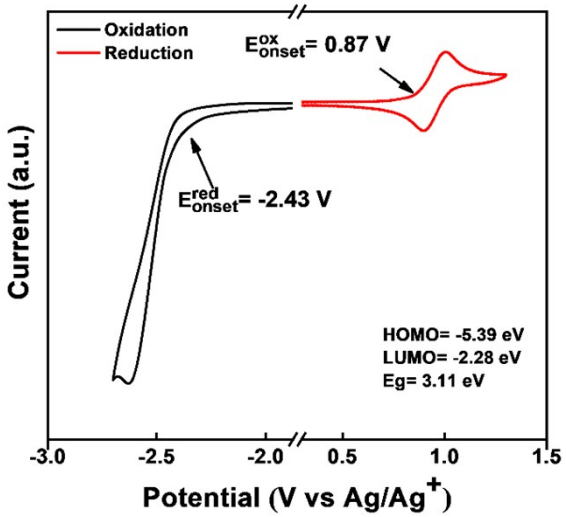


**Figure S5**. CV curve of DTPCZTZ.

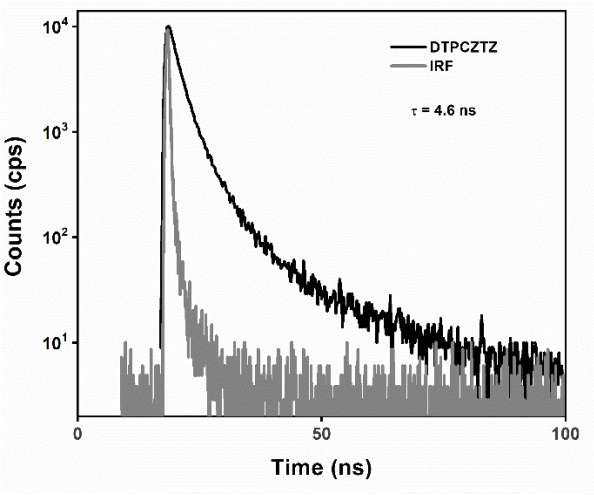


**Figure S6**. Transient spectra in neat film state of DTPCZTZ.

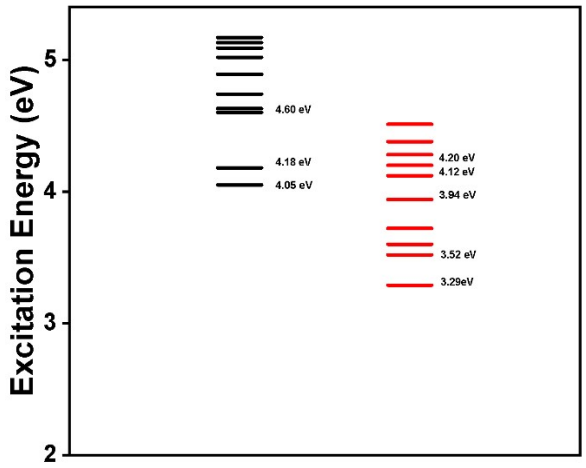


**Figure S7.** The exciton energy levels of DTPCZTZ.

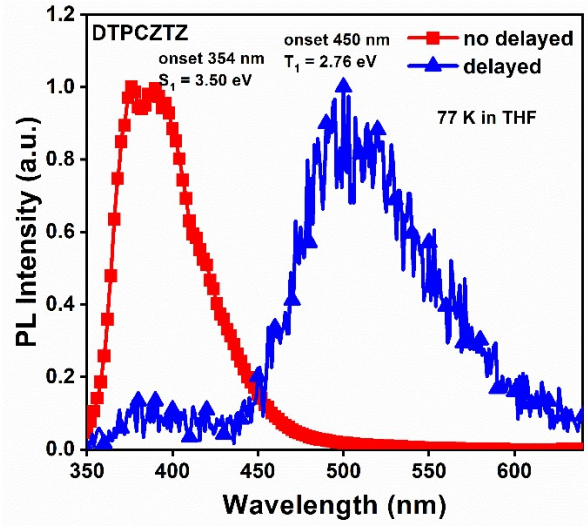


**Figure S8**. The fluorescence and phosphorescence at 77K in THF.

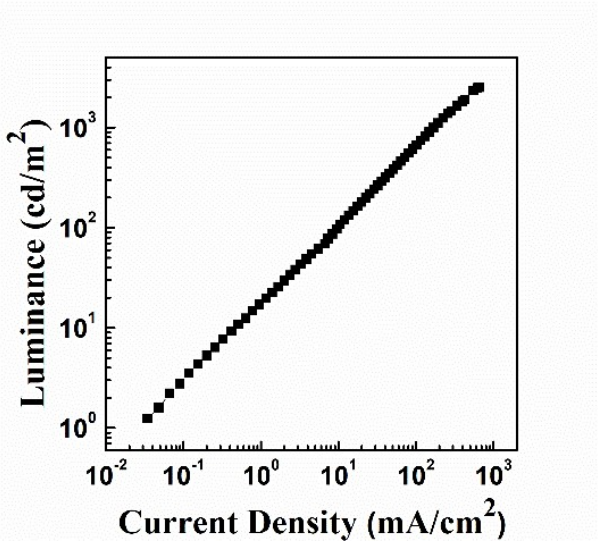


**Figure S9**. The luminance-current density curve of Device-b;

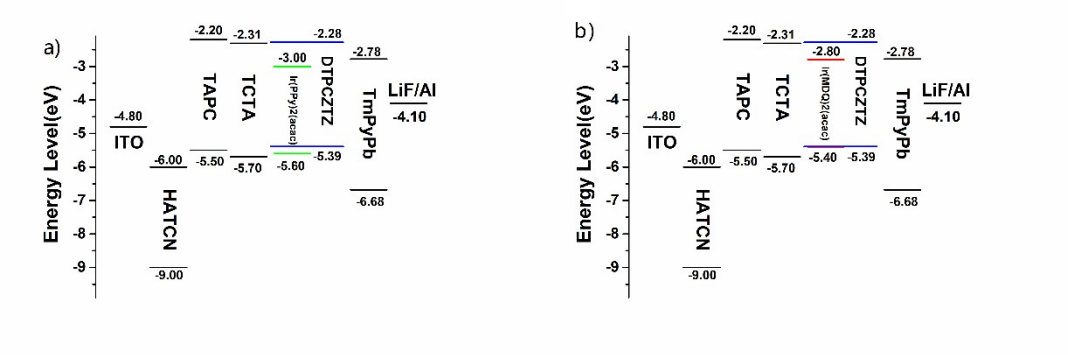


**Figure S10.** The device energy level structure diagram of (a) Device-g and (b) Device-r.

## SI-3 Supporting tables

**Table S1** Single crystal structural parameters of DTPCZTZ.

| Compound | DTPCZPHTZ |
|---|---|
| Chemical formula | C46H42N4 |
| Formula weight | 650.84 |
| Crystal system | Triclinic |
| *a*/Å | a=10.689(6) |
| *b*/ Å | b=12.283(6) |

| | |
|---|---|
| *c*/ Å | c=30.617(16) |
| *α*/° | 86.897(12) |
| *β*/° | 87.912(12) |
| *γ*/° | 66.464(10) |
| Unit cell volume/ Å3 | 3680(3) |
| Temperature/K | 296 K |
| Space group | P -1 |
| Z | 4 |
| Density (calculated) /g $cm^{-3}$ | 1.175 |
| F(000) | 1384.0 |
| Theta range for data collection | 2.49 to 18.49 |
| Index ranges | -12<=h<=12, |
| | -14<=k<=11, |
| | -36<=l<=30 |
| Reflections measured | 19004 |
| Independent reflections | 12854 |
| *Rint* | 0.0797 |
| Completeness to theta = 72.13° | 0.997 |
| Absorption correction | 0.070 |
| Max. and min. transmission | 0.983 and 0.988 |
| Data / restraints / parameters | 12854 / 54 / 901 |
| Goodness-of-fit on $F^2$ | 1.018 |
| Final $R_1$ values ($I> 2\sigma(I)$) | 0.0972 |
| Final $wR(F^2)$ values ($I> 2\sigma(I)$) | 0.1930 |
| Final $R_1$values (all data) | 0.2620 |
| Final $wR(F^2)$ values (all data) | 0.2284 |
| CCDC number | 1985906 |

**Table S2.** The fluorescence quantum efficiency efficiency ($\Phi_{PL}$) of DTPCZTZ in different solvents.

| solvent | n-hexane | isopropyl ether | diethyl ether | tetrahydrofuran | acetonitrile | film |
|---|---|---|---|---|---|---|
| $\Phi_{PL}$(%) | 84.8 | 100 | 90.7 | 85.3 | 72.1 | 57.3 |

**Table S3** EL properties summary of non-doped pure organic deep-blue OLEDs with 400 nm < $\lambda_{EL}$ < 450 nm and $CIE_y$ ~ 0.06 based on organic fluorescent small molecules recently.

| Compound | $V_{on}$ [a] | $CE_{max}$ [b] (cd $A^{-1}$) | $PE_{max}$ [c] (lm $W^{-1}$) | $EQE_{max}$ [d] | $\lambda_{EL}$ | CIE (x, y) | Ref |
|---|---|---|---|---|---|---|---|
| DTPCZTZ | 4.0 | 3.63 | 2.85 | 7.6 | 424 | (0.17,0.06) | This work |
| TPA-(3)-F | - | 0.39 | - | - | 428 | (0.16, 0.06) | [1] |
| PATPA | 3.8 | 0.34 | 0.24 | 0.72 | 424 | (0.15, 0.06) | [2] |
| M2 | | 1.53 | 0.86 | 3.02 | 428 | (0.166, 0.056) | [3] |
| p-DSiTP | 4.0 | 1.11 | 0.79 | 2.7 | 416 | (0.162, 0.061) | [4] |
| P2MPC | 3.1 | 3.42 | 3.36 | 7.15 | | (0.157, 0.064) | [5] |
| PTPC | 3.1 | 2.66 | 2.60 | 6.78 | 411 | (0.156, 0.059) | [6] |
| TPA-PI-SPF | 3.1 | 3.61 | 3.50 | 6.76 | 448 | (0.152, 0.059) | [7] |
| B1 | 3.0 | 1.19 | 1.25 | 5.3 | 406 | (0.16, 0.06) | [8] |
| B2 | 3.2 | 1.39 | 1.25 | 7.1 | 404 | (0.16, 0.06) | [8] |
| TPBCzC2 | 3.4 | 2.01 | 1.57 | 4.78 | 423 | (0.159, 0.06) | [9] |

| | | | | | | | |
|---|---|---|---|---|---|---|---|
| A | 2.8 | 4.12 | 3.2 | 6.4 | 444 | (0.151, 0.066) | [10] |
| 3-CzPOPPI | 2.9 | 2.71 | 2.73 | 5.08 | 436 | (0.156, 0.061) | [11] |
| Ⅰ-A | 3.0 | 5.1 | 5.3 | 8.9 | 444 | (0.15, 0.06) | [12] |
| Ⅰ-B | 2.9 | 5.2 | 5.6 | 8.0 | 444 | (0.149, 0.068) | [12] |
| TPIBCz | 3.0 | 1.7 | 1.44 | 3.38 | 435 | (0.154, 0.063) | [13] |
| B2 | 2.75 | 2.3 | 2.06 | 5.29 | 424 | (0.155, 0.058) | [14] |
| PPi-Xid | 3.3 | 1.94 | - | 3.83 | - | (0.152, 0.057) | [15] |
| PPi-Mid | 3.1 | 2.20 | - | 4.08 | - | (0.154, 0.058) | [15] |
| PPI-2TPA(B) | 3.0 | 2.9 | 3.03 | 4.69 | 442 | (0.15, 0.063) | [16] |
| PPI-2NPA(B) | 3.0 | 2.5 | 2.45 | 4.10 | 448 | (0.152, 0.063) | [16] |

[(a)] Opening voltage [(b)] Maximum current efficiency [(c)] Maximum power efficiency [(d)] Maximum external quantum efficiency [(e)] Emission peak of electroluminescence spectrum

**Reference**

[1] Z. F. Li, Z. X. Wu, W. Fu, P. Liu, B. Jiao, D. D. Wang, G. J. Zhou and X. Hou, Versatile fluorinated derivatives of triphenylamine as hole-transporters and blue-violet emitters in organic light-emitting devices, *J. Phys. Chem. C*, 2012, **116**, 20504-20512.

[2] Y. Zhang, S. L. Lai, Q. X. Tong, M. F. Lo, T. W. Ng, M. Y. Chan, Z. C. Wen, J. He, K. S. Jeff, X. L. Tang, W. M. Liu, C. C. Ko, P. F. Wang and C. S. Lee, High efficiency nondoped deep-blue organic light emitting devices based on imidazole-π-triphenylamine derivatives, *Chem. Mater*, 2012, **24**, 61-70.

[3] Z. Gao, Y. L. Liu, Z. M. Wang, F. Z. Shen, H. Liu, G. N. Sun, L. Yao, Y. Lv, P. Lu and Y. G. Ma, High-efficiency violet-light-emitting materials based on phenanthro[9,10-d]imidazole, *Chem-Eur J*, 2013, **19**, 2602-2605.

[4] Z. Q. Shen, X. Y. Zhu, W. G. Tang, X. J. Feng, Z. J. Zhao and H. Lu, Twisted donor–acceptor molecules for efficient deep blue electroluminescence with CIEy ∼ 0.06, *J.*

*Mater. Chem. C*, 2020, **8**, 9401-9409.

[5] L. Peng, Y. M. Huo, S. Y. He, Y. C. Liu, Z. J. Ren, S. A. Ying and S. K. Yan. A linear deep-blue bipolar fluorescent material with the CIEy ＜ 0.065 serving as the emitter and host for high-performance monochromatic and hybrid white OLEDs, *J. Mater. Chem. C*, 2022, **10**, 11642-11653.

[6] S. A. Ying, J. C. Lv, Y. Z. Li, Y. M. Huo, Y. C. Liu, D. G. Ma, L. Peng and S. K. Yan, A large-scale deep-blue tetraphenylbenzene-bridged hybridized local and charge transfer fluorophore exhibiting small efficiency roll-off and low amplified spontaneous emission threshold, *Mater. Chem. Front*, 2022, **6**, 2085-2094.

[7] S. S. Tang, G. X. Yang, J. J. Zhu, X. He, J. X. Jian, F. Lu and Q. X. Tong, Multifunctional materials serving as efficient non-doped violet- blue emitters and host materials for phosphorescence, *Chem-Eur J*, 2021, **27**, 9102-9111.

[8] Y. Zheng, X. Y. Zhu, Z. G. Ni, X. H. Wang, Z. T. Zhong, X. J. Feng, Z. J. Zhao and H. Lu, Bipolar molecules with hybridized local and charge-transfer state for highly efficient deep-blue organic light-emitting diodes with EQE of 7.4% and CIEy ∼ 0.05, *Adv. Opt. Mater*, 2021, **9**, 2100965.

[9] P. B. Han, C. W. Lin, D. G. Ma, A. J. Qin and B. Z. Tang, Violet-blue emitters featuring aggregation-enhanced emission characteristics for nondoped OLEDs with CIEy Smaller than 0.046, *ACS Appl. Mater. Inter*, 2020, **12**, 46366-46372.

[10] S. F. Ye, Y. X. Wang, R. D. Guo, Q. Zhang, X. L. Lv, Y. L. Duan, P. P. Leng, S. Q. Sun and L. Wang, Asymmetric anthracene derivatives as multifunctional electronic materials for constructing simplified and efficient non-doped homogeneous deep blue fluorescent OLEDs, *Chem. Eng. J*, 2020, 393, 124694.

[11] Z. L. Zhu, S. F. Ni, W. C. Chen, M. Chen, J. J. Zhu, Y. Yuan, Q. X. Tong, F. L. Wong, C. S. Lee, Tuning electrical properties of phenanthroimidazole derivatives to construct multifunctional deep-blue electroluminescent materials, *J. Mater. Chem. C*, 2018, **6**, 3584-3592.

[12] J. S. Huh, Y. H. Ha, S. K. Kwon, Y. H. Kim, J. J. Kim, Design strategy of anthracene-based fluorophores toward high-efficiency deep blue organic light-emitting diodes Utilizing triplet-triplet fusion, *ACS Appl. Mater. Inter*, 2020, **12**, 15422-15429.

[13] W. C. Chen, Y. Yuan, S. F. Ni, Q. X. Tong, F. L. Wong, C. S. Lee. Achieving efficient violet-blue electroluminescence with CIEy ＜ 0.06 and EQE ＞ 4 6% from naphthyl-linked phenanthroimidazole–carbazole hybrid fluorophores, *Chem. Sci*, 2017, **8**, 3599-3608.

[14] Z. Y. Wang, J. W. Zhao, B. Liu, C. Cao, P. Li, Q. X. Tong and S. L. Tao, Universal materials for high performance violet-blue OLEDs (CIEy ＜ 0.06) and PhOLEDs, *Dyes Pigm*, 2019, **163**, 213-220.

[15] J. W. Zhao, B. Liu, Z. Y. Wang, Q. X. Tong, X. Y. Du, C. J. Zheng, H. Lin, S. L. Tao and X. H. Zhang, EQE Climbing Over 6% at High Brightness of 14 350 cd $m^{-2}$ in Deep-Blue OLEDs Based on Hybridized Local and Charge-Transfer Fluorescence, *ACS Appl. Mater. Inter*, 2018, **10**, 9629-9637.

[16] B. Liu, Z. W. Yu, D. He, Z. L. Zhu, J. Zheng, Y. D. Yu, W. F. Xie, Q. X. Tong and C. S. Lee, Ambipolar D–A type bifunctional materials with hybridized local and charge-transfer excited state for high performance electroluminescence with EQE of 7.20% and CIEy ＜ 0.06, *J. Mater. Chem. C*, 2017, **5**, 5402-5410.